Autonomous phagosomal degradation and antigen presentation in dendritic cells

Eik Hoffmann[a,1], Fiorella Kotsias[a,1], Géraldine Visentin[a], Pierre Bruhns[b,c], Ariel Savina[a,2,3], and Sebastian Amigorena[a,2,4]

[a]Institut National de la Santé et de la Recherche Médicale U932, Institut Curie, 75005 Paris, France; [b]Département d'Immunologie, Unité d'Allergologie Moléculaire et Cellulaire, Institut Pasteur, 75015 Paris, France; and [c]Institut National de la Santé et de la Recherche Médicale U760, 75015 Paris, France

Phagocytosis plays a critical role in both innate and adaptive immunity. Phagosomal fusion with late endosomes and lysosomes enhances proteolysis, causing degradation of the phagocytic content. Increased degradation participates in both innate protection against pathogens and the production of antigenic peptides for presentation to T lymphocytes during adaptive immune responses. Specific ligands present in the phagosomal cargo influence the rate of phagosome fusion with lysosomes, thereby modulating both antigen degradation and presentation. Using a combination of cell sorting techniques and single phagosome flow cytometry-based analysis, we found that opsonization with IgG accelerates antigen degradation within individual IgG-containing phagosomes, but not in other phagosomes present in the same cell and devoid of IgG. Likewise, IgG opsonization enhances antigen presentation to CD4$^+$ T lymphocytes only when antigen and IgG are present within the same phagosome, whereas cells containing phagosomes with either antigen or IgG alone failed to present antigen efficiently. Therefore, individual phagosomes behave autonomously, in terms of both cargo degradation and antigen presentation to CD4$^+$ T cells. Phagosomal autonomy could serve as a basis for the intracellular discrimination between self and nonself antigens, resulting in the preferential presentation of peptides derived from opsonized, nonself antigens.

phagosome maturation | IgG ligation | Fcγ receptor | MHC II-restricted presentation

Clearance of pathogens is one of the main functions of phagocytosis, especially in macrophages (MOs) and neutrophils. Signal transduction pathways and actin cytoskeleton-driven rearrangements of the plasma membrane initiate particle engulfment and formation of phagosomes (1). Subsequently, intracellular trafficking and sequential fusion with endosomal and lysosomal compartments enable phagosomes to acquire NADPH oxidases, vacuolar ATPases, and hydrolases to sustain an intraphagosomal milieu with high degradative activity and toxicity for microbes (2). Collectively, this process is termed phagosome maturation. In dendritic cells (DCs), however, phagocytosis serves a different and important function: providing immunogenic peptides for antigen presentation (3). Therefore, the phagocytic and endocytic pathways in DCs are organized to allow effective processing of antigenic peptides. The quantity and activity of proteolytic enzymes in endosomes and phagosomes are decreased compared with MOs (4, 5), whereas the pH in their organelle lumens is also less acidic compared with MOs and neutrophils (6, 7). Overall, DCs have developed a less "aggressive" phagocytic milieu, most likely better suited to preserve peptides destined for antigen presentation from complete degradation.

Physiologically, phagocytosed particles (e.g., bacteria, dead infected cells) contain both antigens and ligands targeting sensors of innate immunity (8). Although innate sensors induce cell activation in all phagocytes, in DCs the situation is more complex (9). Engagement of different receptors, including pattern recognition receptors (PRRs) and IgG receptors (FcγRs), not only induces short-term activation of DCs (10), but also triggers a complex set of developmental modifications that transform DCs into effector cells, capable of presenting antigen and orienting adaptive immune responses.

The control of antigen presentation by innate sensors also has been proposed to serve the discrimination between self and nonself. Antigens that are internalized by DCs in association with innate ligands would be preferentially presented to T cells, compared with self-antigens that reach DCs in the absence of innate signals (11). Whether antigens and PRR or FcR ligands need to be physically present in the same endocytic or phagocytic compartments is unclear, however. Although the results of several studies have favored this possibility, especially in the case of phagocytosed particles (12–14), in most experimental systems it is difficult to distinguish between increased particle uptake and more efficient antigen presentation. The notion that PRR engagement influences phagosomal fate at the single phagosome level (independent of other phagosomes in the same cell), thereby promoting phagosomal-autonomous antigen presentation, has been proposed (15, 16) but remains a matter of debate (17–19). If confirmed, phagosome autonomy could represent a true self/nonself discrimination mechanism at the cellular level, allowing the preferential presentation of PRR- or FcγR-associated antigens over other self-antigens phagocytosed by the same cell.

In the present study, we used ovalbumin (OVA)-coupled latex beads opsonized with IgG, which accelerates phagosomal maturation and promotes antigen presentation (20, 21). Because latex bead phagosomes always contain a single bead, we were able to use a flow cytometry analysis technique on isolated phagosomes from sorted cell populations containing various mixtures of beads bearing different cargo to analyze the autonomy of antigen presentation and phagosome maturation within single DCs and MOs.

Results

Phagosomal Degradation of OVA Is Dependent on IgG Opsonization.
Murine bone marrow-derived DCs and MOs were isolated and cultured as described previously (6). A comparison of their phenotypes revealed the expected differences in expression of CD11c, MHC I, and MHC II molecules, as well as other surface markers (Fig. S1*A*). The used DCs and MOs thus obtained were resting cells, as demonstrated by their different expression of activation markers after LPS treatment of DCs (Fig. S1*B*) or IFN-γ+/− LPS treatment of MOs (Fig. S1*C*). As phagocytic cargo, we used latex beads conjugated to OVA in the presence or absence of opsonic ligand.

We first analyzed OVA degradation in DCs and MOs by fluorescence microscopy. Both cell types efficiently internalized OVA beads into phagosomes that acquire lysosomal-associated membrane protein 1 (LAMP-1) over time, most likely after
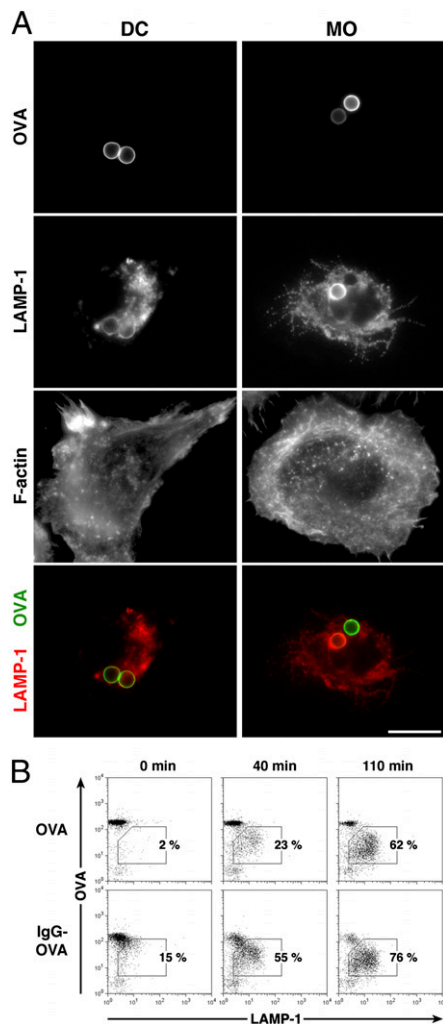
Fig. 1. Phagosomal degradation of OVA is dependent on phagosome maturation kinetics. (*A*) Latex beads conjugated to OVA were internalized by resting bone marrow-derived DCs and MOs and analyzed by high-resolution fluorescence microscopy after labeling of OVA (green), LAMP-1 (red), and F-actin. Shown are maximum projections of five focal planes with a step width of 0.3 μm from representative cells. (Scale bar: 10 μm.) (*B*) DCs were allowed to internalize beads conjugated to OVA or IgG-OVA, and phagosomes were isolated from these cells after different chase times. After simultaneous labeling of OVA and LAMP-1, 5,000 phagosomes of each sample were analyzed by flow cytometry. Results are representative of five independent experiments.

fusion with late endosomes and lysosomes (Fig. 1*A*). As expected, phagosomes highly positive for LAMP-1 were almost devoid of OVA, suggesting a direct link between proteolysis and phago-lysosomal fusion events during phagosome maturation. The observed differences in OVA and LAMP-1 labeling by microscopy were difficult to quantify, however, in part because DCs adhere poorly to glass and grow in clusters.

Consequently, we opted to use a previously developed flow cytometry-based assay, phagoFACS (22, 23), which provides highly quantitative and qualitative measurements, to investigate the rates of OVA degradation and LAMP-1 acquisition simultaneously in individual phagosomes. Both IgG-opsonized and -nonopsonized beads displayed similar amounts of OVA on their surface (Fig. S2*A*, *Upper*). We also verified that IgG was detected only on IgG-OVA beads (Fig. S2*A*, *Lower*). Both types of beads were phagocytosed efficiently by DCs and MOs, as demonstrated by an assay distinguishing intracellular and surface-bound beads (Fig. S2*B*). We found that opsonization of beads with IgG increased the

number of internalized beads per cell when similar numbers of both bead types were used (Fig. S2*C*). The presence of IgG on the beads accelerated both phagosomal degradation of OVA and recruitment of LAMP-1 to phagosomes (Fig. 1*B*). We analyzed the kinetics of OVA degradation and LAMP-1 acquisition in more detail using phagoFACS and found acceleration of both parameters in both DCs and MOs (Fig. 2). MOs exhibited greater proteolytic activity than DCs, but IgG opsonization still induced faster kinetics of OVA degradation and LAMP-1 acquisition in these cells (Fig. 2*B*), as reported previously (24). We also compared OVA beads conjugated to LPS with the other two bead types, to analyze the impact of Toll-like receptor 4 (TLR4) engagement on phagosomal function. In DCs, the presence of LPS increased the kinetics of OVA degradation and LAMP-1 acquisition (Fig. 2*A*), although to a lesser extent than IgG. In contrast, no significant differences between OVA and LPS-OVA beads were observed in MOs (Fig. 2*B*). These results indicate that opsonization of particulate antigens with IgG efficiently accelerates antigen degradation and phagosome maturation.

IgG can bind to several different receptors on the surface of murine DCs that express FcγRI (CD64), FcγRIIB (CD32), and FcγRIII (CD16), but not FcγRIV (25). FcγRI, FcγRIII, and FcγRIV associate to and signal through the FcR-associated γ chain, delivering activation signals through the immunoreceptor tyrosine-based activation motif (ITAM) present in its cytosolic region (21, 26). FcγRIIB bears an immunoreceptor tyrosine-based inhibitory motif that inhibits activation through ITAM-bearing receptors upon co-crosslinking (27). Thus, we investigated whether these receptors are required to accelerate phagosomal degradation in DCs. The increased phagosomal degradation of OVA observed in IgG-OVA phagosomes was lost in DCs from both 5KO mice (deficient in expression of FcγRI, FcγRIIB, and FcγRIII, as well as of FcεRI and FcεRII) (28) and from FcR-associated γ-chain KO mice lacking expression of all IgG receptors except inhibitory FcγRIIB (Fig. S3 *A* and *B*). (Of note, the results shown in Fig. S3 represent only phagocytosed beads.) The results indicate that FcγRIIB expression (in γ-chain KO mice) is not sufficient to mediate accelerated phagosomal maturation that requires the expression of activating IgG receptors FcγRI and/or FcγRIII. These results also exclude the possibility that the observed effects are related to contamination of the beads by other agents (e.g., endotoxins).

Antigen Degradation and Phagosome Maturation Are Regulated Autonomously in DCs and MOs. The results of the foregoing experiments indicate that phagosomal maturation can be analyzed at the single phagosome level. The idea that autonomous phagosome maturation within a single cell underlies autonomous antigen presentation was proposed previously (16); however, the ongoing debate regarding the effect of the engagement of Toll-like receptors on phagosome maturation has challenged this idea (17, 29). To investigate the autonomy of phagosomal fate within single cells, we used OVA and IgG-OVA beads labeled with different dyes added simultaneously to the cells (Fig. S2*D*). We developed a cell sorting strategy to distinguish cell populations containing different combinations and numbers of beads (Fig. S4*A*). Systematic analysis demonstrated that the purity of sorted cell populations exceeded 90% in all experiments.

After different chase periods, cells were sorted and homogenized, and the obtained fraction was labeled and analyzed by phagoFACS. The gating and sorting strategies are shown in Fig. S4*B*. The kinetics of OVA degradation and LAMP-1 recruitment in DCs containing a single phagosome per cell (Fig. 3) were similar to those observed for the bulk population (Fig. 2).

Because the differences in phagosomal fate were more evident with IgG-OVA beads than with LPS-OVA beads, we opted to use the former to assay phagosome autonomy. Autonomy in this experimental setup can be evaluated by comparing the differences between OVA and IgG-OVA phagosomes derived from two separate cells or from the same cell. In DCs, IgG-OVA phagosomes displayed accelerated degradation of OVA over
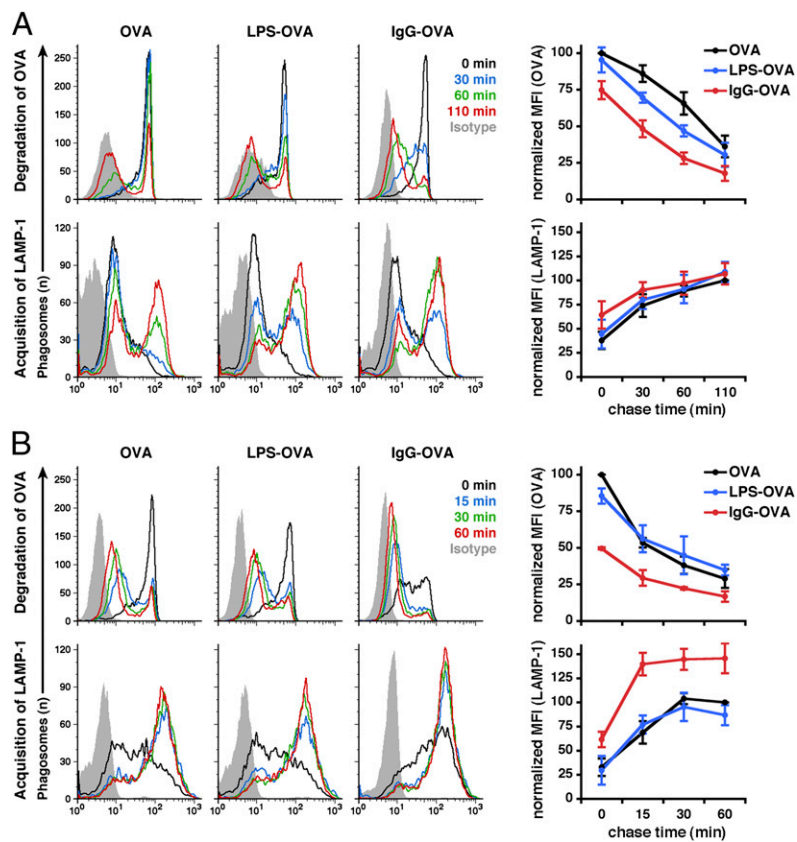
IMMUNOLOGY

www.manaraa.com

Fig. 2. Phagosomes have differing capabilities for degrading OVA and acquiring LAMP-1 depending on the particle ligand. DCs (*A*) and MOs (*B*) were allowed to internalize beads conjugated to OVA, LPS-OVA, and IgG-OVA. Phagosomes were isolated from these cells after different chase times, labeled with antibodies against OVA and LAMP-1, and analyzed by flow cytometry. Results shown are representative of 4,500 analyzed phagosomes labeled for OVA or LAMP-1, as well as isotype controls (gray). The graphs to the right show quantitative data from five independent experiments with DCs (*A*) and three independent experiments with MOs (*B*). The mean fluorescence intensity (MFI) of all samples was normalized to the initial chase time point (OVA degradation) or the final chase time point (LAMP-1 acquisition) of control phagosomes containing OVA beads.

time, independent of any other bead type present in the cell (Fig. 3*A*, *Lower*). Remarkably, OVA phagosomes displayed similarly slow kinetics of OVA degradation regardless of the presence of an IgG-OVA phagosome or of increasing numbers of IgG phagosomes in the same cell (Fig. 3*A*, *Upper*). The presence of additional IgG beads in the same cell slightly accelerated the kinetics of recruitment of LAMP-1 on both phagosome types (Fig. 3*B*), most evident after 40 min of phagocytosis. However, the kinetics of LAMP-1 acquisition to OVA phagosomes (Fig. 3*B*, *Upper*) was still slower than the kinetics of recruitment of LAMP-1 to IgG-OVA phagosomes (Fig. 3*B*, *Lower*). The kinetics of OVA degradation and of LAMP-1 recruitment were faster in MOs than in DCs, but the levels of autonomy were similar in the two types of cells (Fig. S5). Thus, we conclude that the observed acceleration of phagosome maturation on IgG ligation is restricted mostly to the phagosome that actually contains the ligand and does not extend to other phagosomes within the same cell.

Opsonization Enhances Antigen Presentation to CD4+ T Cells. In DCs, IgG opsonization of antigen enhances the efficiency of MHC II-restricted antigen presentation to CD4+ T lymphocytes (12). We analyzed MHC class II presentation to OVA-specific CD4+ T cells (OT-II) after phagocytosis of OVA and IgG-OVA beads in both DCs and MOs. We found that the increase in antigen presentation induced by IgG was less impressive when we used IgG-OVA beads (Fig. 4*A*) than that obtained previously when comparing soluble OVA and OVA immune complexes (12), most likely because OVA bound to beads is already presented more efficiently than soluble OVA. In contrast, MOs did not present OVA efficiently regardless of the presence or absence of IgG on the beads (Fig. 4*A*). Previous studies have shown that in resting conditions, bone marrow-derived MOs express very low levels of MHC class II molecules and require stimulation to become effective antigen-presenting cells (30) (Fig. S1*C*). In agreement with this finding, presentation of the minimal peptide

was completely absent in MOs and highly efficient in DCs (Fig. 4*B*), reflecting the differences in MHC class II expression.

The enhanced antigen presentation observed in DCs with IgG-conjugated beads could be related to either enhanced phagocytosis (Fig. S2*C*) and/or to postphagocytic events triggered by IgG. To analyze antigen presentation in cells that had internalized exactly the same amount of antigen, we used fluorescently labeled beads, as described above, and performed antigen presentation assays with sorted DCs that had phagocytosed a single OVA or IgG-OVA bead. Presentation to OVA-specific OT-II cells was more efficient in DCs containing one IgG-OVA bead compared with those containing one OVA bead, measured either by expression of CD69 (Fig. 4 *C* and *D*) or proliferation of carboxyfluorescein succinimidyl ester (CFSE)-labeled OT-II cells (Fig. 4 *F* and *G*). Phagocytosis of control beads conjugated to BSA or IgG-BSA (without OVA) did not affect presentation of the corresponding minimal peptide added exogenously (Fig. 4 *E* and *H*). The increased antigen presentation obtained with IgG-OVA beads was lost in DCs from 5KO mice and from γ-chain KO mice, suggesting that, similar to phagosome maturation, the increased capacity to present antigens to CD4+ T cells requires FcγRI or III expression by the DCs (Fig. S3 *C*–*E*). We conclude that under strict control of the amount of phagocytosed antigen, IgG opsonization of the beads causes increased MHC II-restricted antigen presentation through engagement of specific FcγRs.

Antigen Presentation by DCs Is Phagosome-Autonomous. To investigate whether one phagosome containing an IgG-conjugated bead increases antigen presentation in other surrounding phagosomes within the same cell, or whether the enhanced antigen presentation is limited to the antigen present in that particular phagosome, we used the same approach as described earlier to isolate cells according to their phagocytic content. We applied two different bead combinations to DCs: (*i*) a mixture of IgG-OVA beads and control BSA beads, with the antigen and the ligand present on the same particle, and (*ii*) a mixture of OVA
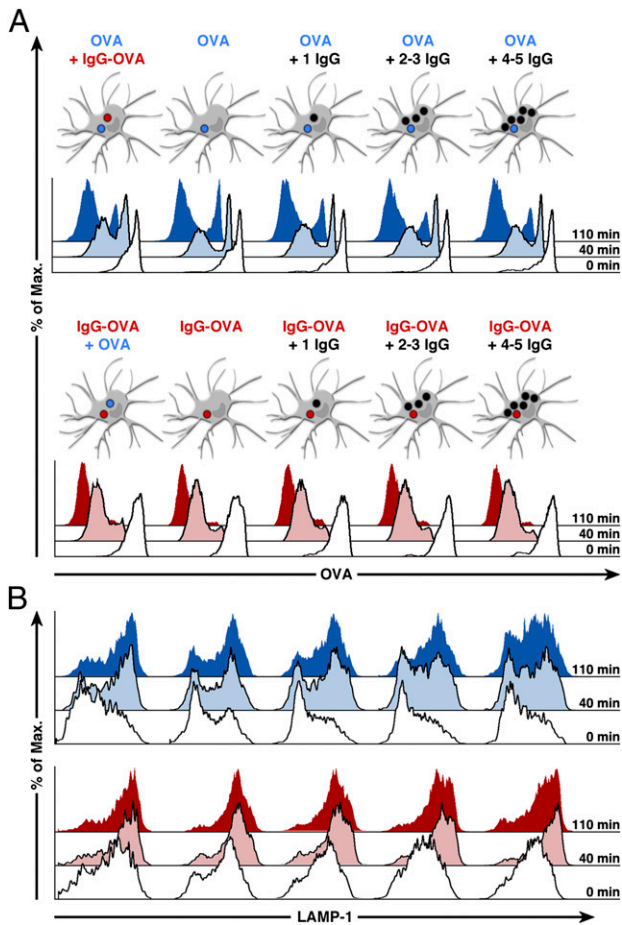
Fig. 3. Phagosome maturation occurs autonomously in DCs. Different mixtures of beads coupled to OVA (blue), IgG-OVA (red), or IgG alone (black) were applied to DCs. The cells were then sorted into different populations, and their phagosomes containing OVA beads (*Upper*) or IgG-OVA beads (*Lower*) were analyzed for phagosomal degradation of OVA (*A*) and phagosomal acquisition of LAMP-1 (*B*) by phagoFACS. Shown are MFI profiles of 3,000 analyzed phagosomes per condition representative of at least five independent experiments.

beads and IgG-BSA beads, with the antigen and the IgG present on separate particles (Fig. 5A). DCs were allowed to phagocytose each of the two mixtures of beads, and the cells were sorted into populations containing either a single bead of either type or two beads, one of each type (Fig. 5A).

As observed earlier, the presence of OVA and IgG on the same bead increased antigen presentation to OVA-specific CD4$^+$ T cells, when antigen presentation was followed by both the induction of CD69 expression (Fig. 5B) and proliferation, as analyzed by CFSE labeling (Fig. 5C). In contrast, the presence of an IgG-BSA bead in a cell that also contained an OVA bead did not increase the level of OT-II stimulation compared with a cell containing a single OVA bead. Moreover, the presence of multiple IgG-BSA beads within the same DC did not influence the efficiency of presentation of OVA in a different phagosome (Fig. S4C). Therefore, when the total amount of antigen per cell is strictly the same, IgG and antigen must be present in the same individual phagosome to enhance antigen presentation. The presence of IgG in a neighboring phagosome within the same cell does not result in enhanced antigen presentation, establishing that phagosomal antigen presentation to CD4$^+$ T lymphocytes in DCs is autonomous.

Discussion

Phagosomes are complex organelles with their own signaling capacities and compositions varying according to their cargo (i.e., phagosome "individuality") (31, 32). Recently, Blander and Medzhitov (16) proposed the idea of phagosomal autonomy, which has
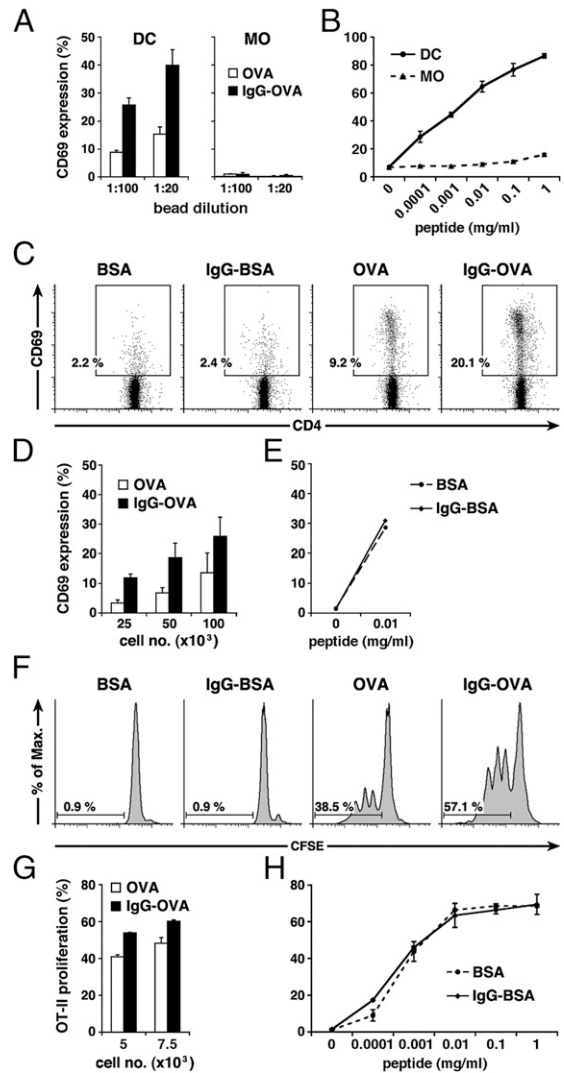

Fig. 4. IgG increases MHC class II-restricted antigen presentation in DCs. (*A*) Beads conjugated to OVA or IgG-OVA were added to DCs or MOs at two different concentrations and cocultured with OT-II lymphocytes to assess MHC II antigen presentation. T-cell activation was examined by FACS analysis of their CD69 surface expression. (*B*) As controls, both cell types were incubated with the synthetic peptide and cocultured with OT-II cells. (*C–H*) Comparable experiments were performed with DCs after phagocytosis of beads conjugated to different ligands and sorted into populations containing only one bead. (*C*) CD69 expression of OT-II cells after coincubation with 100,000 sorted DCs. (*D*) Quantification of OT-II CD69 expression after coincubation with different numbers of sorted DCs and background subtraction. (*E*) As a control, the minimal peptide was added to 50,000 sorted DCs containing one BSA bead or one IgG-BSA bead before OT-II coincubation. (*F–H*) T-cell activation was also assessed using CFSE-labeled OT-II cells. (*F*) Proliferation of OT-II cells after coincubation with 5,000 sorted DCs. (*G*) Quantification of OT-II proliferation after coincubation with 5,000 or 7,500 sorted DCs and background subtraction. (*H*) As a control, the minimal peptide was added to 5,000 sorted DCs containing one BSA bead or one IgG-BSA bead before OT-II coincubation. Representative histograms as well as average data of at least two independent experiments are shown.
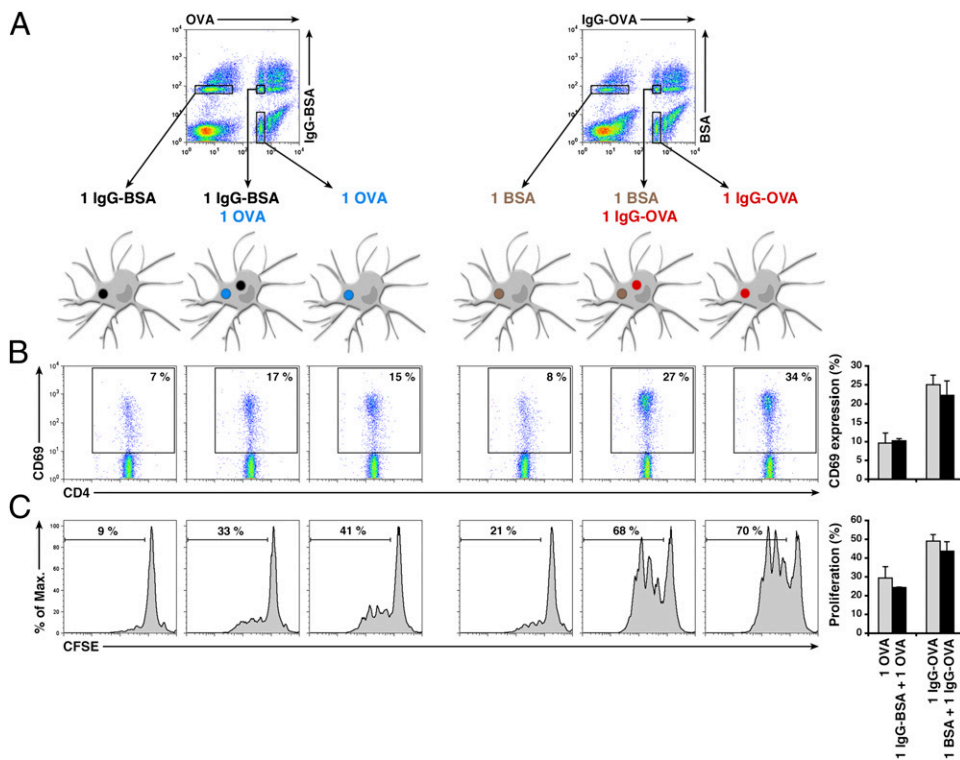
IMMUNOLOGY

Fig. 5. MHC II-restricted presentation of OVA occurs autonomously in DCs. (*A*) Schematic representation of the sorting strategy used for antigen presentation experiments. After simultaneous phagocytosis of different bead types, cells were sorted according to their content into populations containing one of each type or both together within the same cell. (*B*) After sorting and antigen processing, cells were coincubated with OT-II cells and analyzed for expression of CD69. (*C*) The same cells were also coincubated with CFSE-labeled OT-II cells and analyzed for proliferation. Average data as well as representative histograms of three independent experiments are shown.

been supported by results from two elegant studies using engagement of TLR4 by the phagosomal cargo as a model (15, 33). In DCs, the presence of LPS on the same particle as the antigen was found to enhance antigen presentation to CD4$^+$ T cells, whereas an antigen not physically associated to LPS fed to the same DC population was not effectively presented to CD4$^+$ T lymphocytes (15). Based on these findings, the authors proposed the idea that phagosomes behave autonomously within single cells, and that this autonomy serves as a basis for self/nonself discrimination. The fact that phagosomes can behave autonomously in terms of antigen presentation is based mechanistically on the assumption that the efficacy of phagosomal maturation is influenced by phagosome cargo. Thus, the controversy regarding the effect of LPS on phagosomal maturation (17–19) calls into question the concept of phagosomal autonomy proposed using LPS-coated phagosome cargos.

Why different studies have obtained different results when measuring the effect of LPS on phagosomal fate is unclear. Blander and Medzhitov (15) used confocal microscopy to colocalize phagocytosed particles with late endosomal/lysosomal markers (lysotracker or LAMP-1). This technique is based on visual quantification, which can be delicate and sometimes misleading. In contrast, the methods used by Russell and Yates (29) are based on ratiometric fluorimetry, a much more quantitative and reliable approach. Nevertheless, this method quantifies the fate of a complete population of fluorescent beads regardless of their internalization and distribution across the cell population. This can be a concern with DCs, which are very inefficient at phagocytosis compared with MOs. Minor contaminations of the DC population with undifferentiated monocytes or MOs (which are highly phagocytic compared with DCs) could account for a large proportion of the phagocytosed beads. In our experiments, the effect of LPS on phagosome maturation was not very strong in DCs and was absent in MOs (which have very high levels of phagosome maturation compared with DCs). It is also impossible to exclude the possibility that these in vitro-generated populations have different characteristics depending on the culture conditions used in different laboratories. Our methodology is fully quantitative and allows us to follow only beads present inside cells, as well as to assay surface markers (e.g., CD11c) on the cells that have phagocytosed the beads.

Our study used an experimental cargo widely accepted to direct phagosomal maturation (IgG) in MOs and, as we show here, in DCs as well. We measured phagosomal autonomy quantitatively and unambiguously. In the case of LPS, we found only a modest increase in the rate of phagosomal OVA degradation using bulk DC populations (Fig. 2). Thus, the differences between OVA and OVA-LPS beads were too small to allow us to analyze phagosomal autonomy unambiguously in our model system (in which sorted cells containing a single bead are used). Nevertheless, in the case of IgG, our results on antigen degradation and presentation show that phagosomes can behave as individual functional entities independent of other phagosomes in the same cell. In certain cases (e.g., for phagosomal acquisition of LAMP-1), phagosomes within single cells also can influence one another, suggesting the existence of molecular crosstalk between phagosomes carrying different cargos. Unraveling the molecular mechanism involved in this process will allow investigation of the functional relevance of phagosome autonomy, including the immunological distinction between self and nonself.

Materials and Methods

Cell Generation. Bone marrow-derived DCs and MOs were produced by culture in GM-CSF–containing medium (6, 34) and in M-CSF–containing medium (35), respectively. Activation of cells was induced by a 16-h treatment with 1 μg/mL of LPS from *Salmonella enterica enterica*, serovar Typhimurium (Sigma-Aldrich) alone or in combination with 10 ng/mL of IFN-γ (R&D Systems).

CD4$^+$ OT-II cells specific for the OVA$_{323–339}$ peptide in a I-A^b MHC class II context were obtained from lymph nodes of OT-II mice and isolated using negative selection (Miltenyi Biotec) in accordance with the manufacturer's instructions.

Phagocytosis Assays and Cell Sorting. Cells were collected from culture dishes, washed once in PBS, and resuspended in CO$_2$-independent medium (Invitrogen) at a density of 20 × 10^6 cells/mL. Phagocytic binding and uptake of beads to the cell suspension was performed in 15-mL tubes for 10 min at 4 °C, followed by different chase times at 37 °C (for phagocytic uptake experiments), 25 min at 16 °C followed by 5 min at 37 °C (for phagoFACS experiments), or 15 min at 16 °C followed by 15 min at 37 °C (for antigen presentation experiments). Pulse periods were stopped by the addition of 10 mL of ice-cold PBS. After cells were pelleted, noninternalized beads were

Hoffmann et al.

removed by two washes in ice-cold PBS after the tubes were shaken vigorously, followed by one run of the cell suspension overlaid on top of 5 mL of FCS at $150 \times g$ for 4 min at 4 °C. Cells were resuspended in complete medium and incubated at 37 °C for different chase periods. Subsequently, some samples were sorted immediately after the pulse or different chase periods according to their phagocytic content using a BD FACSVantage SE cell sorter. To distinguish external from internalized beads, samples containing OVA or IgG-OVA beads were labeled with an OVA antibody and appropriate fluorescently labeled secondary antibodies before proceeding with cell sorting and/or the different approaches.

Flow Organellocytometry (phagoFACS). The flow cytometry techniques used to analyze the capacity of phagosomes to degrade proteins and acquire LAMP-1 have been described previously (23). In brief, after phagocytosis assays, cells were washed in cold PBS and resuspended in homogenization buffer [3 mM imidazole (pH 7.4), 250 mM sucrose, 2 mM DTT, 2 mM phenylmethylsulfonyl fluoride, 2× protease inhibitor mixture; Roche]. Subsequently, cells were disrupted mechanically with 2-mL syringes and 22-gauge needles (Terumo Medical). Intact cells and nuclei were removed by centrifugation at $150 \times g$ for 4 min at 4 °C, after which postnuclear supernatant was transferred to 96-well conical-bottomed microplates (Greiner Bio-One). Nonspecific binding sites were blocked by incubation in PBS/1% (vol/vol) BSA, followed by labeling on ice using the aforementioned antibodies against OVA, IgG, and LAMP-1 and appropriate secondary antibodies. Samples were analyzed with a BD FACSCalibur unit, with gating on bead-containing phagosomes and their ligand-specific dyes. A minimum of 2,000 events for each ligand type and time point were analyzed using FlowJo software (Tree Star) for profiles of labeled OVA and LAMP-1 in each experiment.

Antigen Presentation Experiments. For these experiments, 5×10^4 DCs or MOs were incubated at 37 °C on 96-well round-bottomed plates with different amounts of 3-μm-diameter latex amino beads covalently conjugated to OVA, BSA, and/or IgG for 5 h in complete medium. Cells incubated with different concentrations of MHC class II (OVA$_{323-339}$) minimal peptides (PolyPeptide Laboratories) were included as a control of the surface amount of MHC class II molecules.

For antigen presentation experiments using DCs that internalized only one bead, cells were pulsed as described above at a ratio of 10 beads per cell and sorted. After cell counting, DCs were plated in different numbers onto 96-well round-bottomed plates and incubated in complete medium at 37 °C for 5 h. In addition, sorted DCs that had phagocyted one BSA bead or one IgG-BSA bead were incubated with the minimal peptide to control the surface amount of MHC molecules.

For phagosome autonomy experiments, cells were allowed to internalize two different bead types, each labeled with a different dye (Alexa Fluor 488 or Alexa Fluor 647) during a 30-min pulse and sorted for the populations that had internalized only one type of bead or both types simultaneously. Then cells were plated and chased for 5 h as described above.

In all cases, after three washes with PBS containing 0.1% BSA, cells were fixed with 0.008% glutaraldehyde and cocultured with 10^5 T cells for 18 h. OT-II cell activation was assessed by FACS analysis of CD69 expression of the CD4$^+$ T-cell population. Alternatively, cells were chased for 2 h, and 10^5 CFSE-labeled OT-II CD4$^+$ T cells were added to each well. After 3 d, proliferation was examined by FACS analysis of the percentage of TCR-β chain-positive cells exhibiting decreased CFSE fluorescence intensity.

1. Swanson JA (2008) Shaping cups into phagosomes and macropinosomes. *Nat Rev Mol Cell Biol* 9:639–649.
2. Kinchen JM, Ravichandran KS (2008) Phagosome maturation: Going through the acid test. *Nat Rev Mol Cell Biol* 9:781–795.
3. Savina A, Amigorena S (2007) Phagocytosis and antigen presentation in dendritic cells. *Immunol Rev* 219:143–156.
4. Lennon-Duménil AM, et al. (2002) Analysis of protease activity in live antigen-presenting cells shows regulation of the phagosomal proteolytic contents during dendritic cell activation. *J Exp Med* 196:529–540.
5. Delamarre L, Pack M, Chang H, Mellman I, Trombetta ES (2005) Differential lysosomal proteolysis in antigen-presenting cells determines antigen fate. *Science* 307:1630–1634.
6. Savina A, et al. (2006) NOX2 controls phagosomal pH to regulate antigen processing during crosspresentation by dendritic cells. *Cell* 126:205–218.
7. Savina A, et al. (2009) The small GTPase Rac2 controls phagosomal alkalinization and antigen crosspresentation selectively in CD8(+) dendritic cells. *Immunity* 30:544–555.
8. Blander JM, Sander LE (2012) Beyond pattern recognition: Five immune checkpoints for scaling the microbial threat. *Nat Rev Immunol* 12:215–225.
9. Reis e Sousa C (2006) Dendritic cells in a mature age. *Nat Rev Immunol* 6:476–483.
10. Stuart LM, Ezekowitz RA (2005) Phagocytosis: Elegant complexity. *Immunity* 22:539–550.
11. Ishii KJ, Koyama S, Nakagawa A, Coban C, Akira S (2008) Host innate immune receptors and beyond: Making sense of microbial infections. *Cell Host Microbe* 3:352–363.
12. Regnault A, et al. (1999) Fcgamma receptor-mediated induction of dendritic cell maturation and major histocompatibility complex class I-restricted antigen presentation after immune complex internalization. *J Exp Med* 189:371–380.
13. Inaba K, et al. (2000) The formation of immunogenic major histocompatibility complex class II-peptide ligands in lysosomal compartments of dendritic cells is regulated by inflammatory stimuli. *J Exp Med* 191:927–936.
14. Fujii S, Liu K, Smith C, Bonito AJ, Steinman RM (2004) The linkage of innate to adaptive immunity via maturing dendritic cells in vivo requires CD40 ligation in addition to antigen presentation and CD80/86 costimulation. *J Exp Med* 199:1607–1618.
15. Blander JM, Medzhitov R (2006) Toll-dependent selection of microbial antigens for presentation by dendritic cells. *Nature* 440:808–812.
16. Blander JM, Medzhitov R (2006) On regulation of phagosome maturation and antigen presentation. *Nat Immunol* 7:1029–1035.
17. Russell DG, Yates RM (2007) Toll-like receptors and phagosome maturation. *Nat Immunol* 8:217–author reply 217–218.
18. Blander JM (2007) Signalling and phagocytosis in the orchestration of host defence. *Cell Microbiol* 9:290–299.
19. Russell DG, Yates RM (2007) TLR signalling and phagosome maturation: An alternative viewpoint. *Cell Microbiol* 9:849–850.
20. Manca F, Fenoglio D, Li Pira G, Kunkl A, Celada F (1991) Effect of antigen/antibody ratio on macrophage uptake, processing, and presentation to T cells of antigen complexed with polyclonal antibodies. *J Exp Med* 173:37–48.
21. Amigorena S, Salamero J, Davoust J, Fridman WH, Bonnerot C (1992) Tyrosine-containing motif that transduces cell activation signals also determines internalization and antigen presentation via type III receptors for IgG. *Nature* 358:337–341.
22. Ramachandra L, Sramkoski RM, Canaday DH, Boom WH, Harding CV (1998) Flow analysis of MHC molecules and other membrane proteins in isolated phagosomes. *J Immunol Methods* 213:53–71.
23. Savina A, Vargas P, Guermonprez P, Lennon AM, Amigorena S (2010) Measuring pH, ROS production, maturation, and degradation in dendritic cell phagosomes using cytofluorometry-based assays. *Methods Mol Biol* 595:383–402.
24. Oh YK, Swanson JA (1996) Different fates of phagocytosed particles after delivery into macrophage lysosomes. *J Cell Biol* 132:585–593.
25. Bruhns P (2012) Properties of mouse and human IgG receptors and their contribution to disease models. *Blood* 119:5640–5649.
26. Bonnerot C, et al. (1992) Role of associated gamma-chain in tyrosine kinase activation via murine Fc gamma RIII. *EMBO J* 11:2747–2757.
27. Amigorena S, et al. (1992) Cytoplasmic domain heterogeneity and functions of IgG Fc receptors in B lymphocytes. *Science* 256:1808–1812.
28. Mancardi DA, et al. (2008) FcgammaRIV is a mouse IgE receptor that resembles macrophage FcepsilonRI in humans and promotes IgE-induced lung inflammation. *J Clin Invest* 118:3738–3750.
29. Yates RM, Russell DG (2005) Phagosome maturation proceeds independently of stimulation of toll-like receptors 2 and 4. *Immunity* 23:409–417.
30. Fischer HG, Frosch S, Reske K, Reske-Kunz AB (1988) Granulocyte-macrophage colony-stimulating factor activates macrophages derived from bone marrow cultures to synthesis of MHC class II molecules and to augmented antigen presentation function. *J Immunol* 141:3882–3888.
31. Griffiths G (2004) On phagosome individuality and membrane signalling networks. *Trends Cell Biol* 14:343–351.
32. Hoffmann E, et al. (2010) Initial receptor-ligand interactions modulate gene expression and phagosomal properties during both early and late stages of phagocytosis. *Eur J Cell Biol* 89:693–704.
33. Blander JM, Medzhitov R (2004) Regulation of phagosome maturation by signals from toll-like receptors. *Science* 304:1014–1018.
34. Winzler C, et al. (1997) Maturation stages of mouse dendritic cells in growth factor-dependent long-term cultures. *J Exp Med* 185:317–328.
35. Al-Haddad A, et al. (2001) Myosin Va bound to phagosomes binds to F-actin and delays microtubule-dependent motility. *Mol Biol Cell* 12:2742–2755.

IMMUNOLOGY

Hoffmann et al.